

J/ψ suppression at forward rapidity as a potential probe for QGP formation in colour screening scenario

M. Mishra¹, C. P. Singh² and V. J. Menon

Department of Physics, Banaras Hindu University, Varanasi 221005, India

Abstract

In order to study the properties of J/ψ in the deconfining medium, we extend our previous formalism [Phys. Lett. B **656** (2007) 45] on J/ψ suppression using colour screening framework. Our formalism is more general as the complete rapidity and centrality dependence including J/ψ suppression at forward as well as mid-rapidity can be computed directly from it. Careful attention is paid to the role of the medium's proper time in determining the locus of the deadly region where J/ψ gets killed. Other important ingredients in the calculation are bag model equation of state for QGP, the longitudinal expansion of the QGP fluid obeying Bjorken's boost invariant scaling law and sequential melting of χ_c (1P) and ψ' (2S) higher resonances. On comparison with the recent data of PHENIX collaboration on J/ψ suppression at forward and mid-rapidity regions, we find that our model shows a reasonable agreement with the data. Furthermore, we observe a larger suppression at forward rapidity in our model which is again well supported by the PHENIX data.

PACS numbers: 25.75.-q; 25.75.Nq; 12.38.Mh; 25.75.Gz

Keywords: J/ψ suppression, Survival probability, Sequential melting, Relativistic heavy-ion collisions, Colour Debye screening.

¹Email: madhukar.12@gmail.com

²Email: cpsingh_bhu@yahoo.co.in

1 Introduction

The current experimental programmes at RHIC are focused towards the investigations of the properties of hadrons or hadronic resonances above the deconfinement transition. In particular, suppression of J/ψ (or charmonium state) has been suggested as a potential probe of the deconfined matter produced in the ultra-relativistic heavy-ion collisions. Lattice quantum chromodynamics (QCD) calculations reveal that the critical temperature for confined normal nuclear matter (HG) to deconfined matter (QGP) phase transition is $T_c \sim 0.160 - 0.190$ GeV if a baryonic chemical potential $\mu_B = 0$ [1]. Matsui and Satz [2] first predicted that the binding potential of the $c\bar{c}$ pair into J/ψ mesons is screened in the presence of a QGP medium and J/ψ states dissociate at temperatures for which the colour (Debye) screening radius of the medium falls below their corresponding $c\bar{c}$ binding radius. The strength of the suppression depends on the binding energies of the quarkonia and the temperature of the medium [2]. Recent lattice QCD calculations show that J/ψ can survive in a QGP at temperatures up to about $2T_c$ [3, 4]. This also means that J/ψ can survive upto the energy density $\epsilon \approx 16\epsilon_c$ where the critical energy density $\epsilon_c \approx 1$ GeV/fm³. However, the higher resonances, such as χ_c (1P) and ψ' can still melt near T_c . Relativistic heavy-ion collision experiments can produce deconfined state of matter, J/ψ and their higher resonances are created at the initial (pre-thermal) stage of heavy-ion collisions because of their large masses. Their small widths also make them insensitive to final state interactions. Therefore, their J/ψ particles probe the evolution of the deconfined state of matter from the early stage of collisions [5].

There are now high-statistics data available for J/ψ suppression obtained by NA50 experiments [6, 7, 8] at SPS and by PHENIX experiments at RHIC [9]. One of the surprising result is the observation of a similar suppression pattern at both these energies involving a large difference in the energy densities being produced between SPS and RHIC. The other important feature of the PHENIX J/ψ suppression data in Au+Au collisions at the center-of-mass energy $\sqrt{s_{NN}} = 200$ GeV at RHIC is that J/ψ yield in the central Au+Au collisions is suppressed by a factor of nearly 4 at mid-rapidity and 5 at forward rapidity as compared to that in p+p collisions scaled by the average number of binary collisions. Two types of models have been developed to explain the above result. In one type of models, one considers that χ_c (1P) and ψ' (2S) states evaporate shortly above T_c while J/ψ (1S) survives upto the temperatures reached at RHIC experiments. Thus the J/ψ suppression mostly results due to the depletion of χ_c and ψ' resonances in the QGP scenario. In other type of models, it is assumed that J/ψ yield will result from a balance between annihilation of J/ψ due to thermal gluons [10, 11] along with colour screening [12, 13] and enhancement due to coalescence of uncorrelated $c\bar{c}$ pairs [14, 15, 16] which are produced abundantly at RHIC energy [17, 18]. However, PHENIX data do not show any indication of J/ψ enhancement. Cold nuclear matter (CNM) effects such as nuclear absorption, shadowing and anti-shadowing are also expected to modify the J/ψ yield. CNM effects due to the gluon shadowing and nuclear absorption of J/ψ at the RHIC energy were evaluated from the J/ψ measurement in d+Au collisions at RHIC [19]. PHENIX data on the centrality dependence of J/ψ suppression have already been analyzed by several models such as comover model [20], statistical coalescence model [21, 22], kinetic model [14], statistical hadronization model [23] and QCD based nuclear absorption model [24]. None of these models give

the satisfactory description of the present experimental data. In particular, we do not find any single mechanism which can be used to explain the complete rapidity dependence of the J/ψ suppression. Chaudhuri has attempted to explain the forward-rapidity suppression [25] in a QGP motivated threshold model supplemented with normal nuclear absorption. However, this appears more like a parameter fitting because the parameters used in the analysis (e.g., QGP formation time $\tau = 0.06 - 0.08$ fm/c) do not convey any physical meaning. Moreover, in order to accommodate rapidity dependence in the formulation he considers three parameters used in the analysis e.g., J/ψ nuclear absorption cross-section, threshold density and its smearing factor λ to explicitly depend on the rapidity variable. Similarly Gunji et al. [26] have recently used a hydro+ J/ψ model in which QGP has been considered as undergoing (3+1)-dimensional hydrodynamic expansion but it has been used to explain the mid-rapidity data alone. Recently, we have analyzed PHENIX data of J/ψ suppression, normalized by normal nuclear matter suppression factor [26, 27, 28], by using a modified colour screening model of Chu and Matsui [13]. Moreover, we have taken a bag model equation of state and (1+1)-dimensional hydrodynamic evolution for QGP as well as additional time dilatation effect for charmonium. We find that it describes the centrality dependence of J/ψ suppression at mid-rapidity quite well [12].

In this paper, we have generalized the above geometric formulation in order to incorporate the rapidity dependence by explicitly introducing rapidity variable in a consistent manner. Here again we consider (1+1)-dimensional hydrodynamic evolution of the QGP and the sequential dissociation scenario for the charmonium excited states. Our theory emphasizes the role of the medium's proper time in finding the locus of the deadly region and also gives a prescription for estimating the length of the primordial cylinder in which $c\bar{c}$ pairs were created. We predict the centrality (i.e., impact parameter or number of participant nucleons N_{part}) dependence of the J/ψ suppression in Au+Au collisions at mid-rapidity as well as at forward rapidity and compare with the experimental data observed by PHENIX collaboration at RHIC. We notice that our model reproduces the main features of the data quite well. We have also found that the present model gives more J/ψ suppression at forward rapidity than that at mid-rapidity and this fact is again in quite good agreement with the recent PHENIX data.

2 Formulation

Although our basic theme is similar to that described in refs. [12, 13] yet, for the sake of convenience, we briefly recapitulate it below and also point out the important differences at appropriate places. For a QGP with massless quarks and gluons, the bag model EOS gives [12, 29]:

$$\begin{aligned} \epsilon &= aT^4/c_s^2 + B \quad ; \quad P = aT^4 - B \sim a(T^4 - T_c^4); \\ c_s^2 &\equiv \frac{\partial P}{\partial \epsilon} \quad ; \quad a \equiv \frac{37\pi^2}{90} \quad ; \quad B \equiv \frac{17\pi^2 T_c^4}{45} \sim aT_c^4, \end{aligned} \tag{1}$$

where at every time-space point $x \equiv (t, \vec{x})$, ϵ is the energy density, P the pressure, T_c the critical temperature, c_s^2 the square of velocity of sound, the coefficient a describes the number

of degrees of freedom, and B is the bag constant. It should be added here that the bag model EOS exhibits a first order phase transition between the QGP and the HG phases which is not well supported by the recent lattice QCD simulations. Even though the bag model EOS has been often used for hydrodynamic calculations, it should be understood as a convenient way of parameterizing some features of the EOS with rapid change of entropy density as a function of temperature in the transition region. For a QGP undergoing (1+1)-dimensional Bjorken's boost invariant expansion, the local thermodynamic observables become function of the lateral coordinate r along with the proper time $\tau \equiv (t^2 - z^2)^{1/2}$, so that the cooling laws become

$$\tilde{\epsilon} = \tilde{P} = \tilde{T}^4 = \tilde{\tau}^{-q} \quad ; \quad q \equiv 1 + c_s^2, \quad (2)$$

where the dimensionless symbols $\tilde{\tau} \equiv \tau/\tau_i$, $\tilde{T} \equiv T(\tau, r)/T(\tau_i, r)$, $\tilde{\epsilon} \equiv (\epsilon(\tau, r) - B)/(\epsilon(\tau_i, r) - B)$ and $\tilde{P} \equiv (P(\tau, r) + B)/(P(\tau_i, r) + B)$, have been introduced for convenience with τ_i being the proper time for initial thermalization of the fireball.

From (1) the pressure is seen to almost vanish at the transition point T_c , i.e., in the hadronic sector. Hence on any transverse plane we choose the initial pressure profile

$$P(\tau_i, r) = P(\tau_i, 0) h(r) \quad ; \quad h(r) \equiv \left(1 - \frac{r^2}{R_T^2}\right)^\beta \theta(R_T - r), \quad (3)$$

where R_T denotes the radius of the cylinder. The power β depends on the energy deposition mechanism, and θ is the unit step function. Clearly, our pressure is maximum at the center of the plasma but vanishes at the edge R_T where hadronization occurs. The factor $P(\tau_i, 0)$ is related to the mean pressure $\langle P \rangle_i$ over the cross-section and to the corresponding average initial energy density $\langle \epsilon \rangle_i$ via

$$P(\tau_i, 0) = (1 + \beta) \langle P \rangle_i = (1 + \beta) \{c_s^2 \langle \epsilon \rangle_i - q B\}. \quad (4)$$

In the present work, we take the initial average energy density $\langle \epsilon \rangle_i$ in terms of the number of participating nucleons N_{part} [27] (which depends on the impact parameter b), given by the modified Bjorken formula:

$$\langle \epsilon \rangle_i = \frac{\xi}{A_T \tau_i} \left(\frac{dE_T}{dy_H} \right)_{y_H=0} \quad ; \quad A_T = \pi R_T^2, \quad (5)$$

where A_T is the transverse overlap area of the colliding nuclei and $(dE_T/dy_H)_{y_H=0}$ is the transverse energy deposited per unit rapidity of output hadrons. Both depend on the number of participants N_{part} [31] and thus provide centrality dependent initial average energy density $\langle \epsilon \rangle_i$ in the transverse plane. The phenomenological scaling factor ξ discussed latter in Sec. 3 in conjunction with the self-screened parton cascade model.

It is well known that $c\bar{c}$ bound state in a thermal medium feels a colour screened Yukawa potential and it melts at the dissociation temperature T_D (determined by recent Lattice QCD simulations) which corresponds to the energy density ϵ_s and pressure P_s given by

$$T_D \geq T_c \quad ; \quad \epsilon_s = a T_D^4 / c_s^2 + B \quad ; \quad P_s = a T_D^4 - B. \quad (6)$$

For any chosen fireball instant t and on the arbitrary z plane the contour of constant pressure P_s is obtained by combining the cooling laws (3) with the profile shape (4) to yield

$$\tilde{P} \equiv \frac{P_s + B}{P(\tau_i, 0) h(r) + B} = \tilde{\tau}^{-q}. \quad (7)$$

Setting $r = 0$ the maximum allowed tilde time $\tilde{\tau}_{s0}$ (during which pressure drops to P_s at the center) can be identified as

$$\tilde{\tau}_{s0} \equiv \left\{ \frac{P(\tau_i, 0) + B}{P_s + B} \right\}^{1/q}, \quad (8)$$

with $P(\tau_i, 0)$ read-off from (4). Thereby the said locus takes the more convenient form

$$\left(1 - \frac{r^2}{R_T^2}\right)^\beta = H_s(\tau) \equiv \frac{\tilde{\tau}^q - B/(P_s + B)}{\tilde{\tau}_{s0}^q - B/(P_s + B)}. \quad (9)$$

Our above result generalizes a similar expression derived by us [12] for the special case when the transverse plane pass through the origin and the proper time was t itself.

Next, consider an interacting $c\bar{c}$ pair created at the early time $t_1 \sim \hbar/2m_c \approx 0$ at the location (r_1, ϕ_1, z_1) inside a cylinder of length L_1 . The precise value of L_1 is not known a priori since different physical arguments can give different results, among which a recipe exploiting rapidity will turn out to be logical as discussed in the numerical section. The $c\bar{c}$ pair has mass m , transverse momentum p_T , transverse mass $m_T = \sqrt{m^2 + p_T^2}$, rapidity y , total energy $p^0 = m_T \cosh(y)$, longitudinal momentum $p_z = m_T \sinh(y)$, vectorial velocity $\vec{v} = (\vec{p}_T + \vec{p}_z)/p^0$ and dilation factor $\gamma = p^0/m$. In the fireball frame the pair will convert itself into the physical J/ψ resonance after the lapse of time $t = \gamma \tau_F$ (with τ_F being the intrinsic formation time) provided the temperature $T < T_D$. At this instant the pair's transverse position \vec{r} , its longitudinal position z and medium's proper time τ are given by

$$\begin{aligned} \vec{r} &= \vec{r}_1 + v_T t \quad ; \quad z = z_1 + v_z t \\ \tau &= (t^2 - z^2)^{1/2} \theta(t - |z|) \quad ; \quad t \equiv \gamma \tau_F. \end{aligned} \quad (10)$$

From the locus (9) we deduce the so called screening radius

$$r_s = R_T \{1 - H_s^{1/\beta}(\tau)\}^{1/2} \theta\{1 - H_s(\tau)\}. \quad (11)$$

In contrast to the earlier paper [12], the important role of proper time τ and hence of the longitudinal velocity v_z must be noted in the definition of the screening radius r_s , which marks the boundary of the circular region where the quarkonium formation is prohibited. Since τ and hence $H_s(\tau)$ decreases as $|v_z|$ increases, it is clear that the radius r_s of the deadly region grows with growing longitudinal speed. This fact will be utilized for interpreting our graphical results in Sec. 4.

Due to the existence of the deadly region the pair will escape and form quarkonium if $|\vec{r}_1 + \vec{v}_T t| \geq r_s$ implying

$$\cos(\phi_1) \geq Y \quad ; \quad Y \equiv \frac{[(r_s^2 - r_1^2) - v_T^2 t^2]}{2 r_1 t |v_T|}, \quad (12)$$

where the roll of the transverse velocity v_T has become explicit. This trigonometric inequality is equivalent to saying that $-\phi_{max}(r_1, z_1) \leq \phi_1 \leq \phi_{max}(r_1, z_1)$ where

$$\phi_{max}(r_1, z_1) = \begin{cases} \pi & \text{if } Y \leq -1, \\ \pi - \cos^{-1} |Y| & \text{if } -1 \leq Y \leq 0, \\ \cos^{-1} |Y| & \text{if } 0 \leq Y \leq 1, \\ 0 & \text{if } Y \geq 1. \end{cases}$$

In contrast to our earlier work [12] the symbol ϕ_{max} depends on both r_1 and z_1 .

Finally, we must deal with the anomalous survival probability due to QGP effect namely, $S(N_{part}, p_T, y)$. Suppose the overall probability distribution for the production of $c\bar{c}$ pair at general position with general momentum is factorized as $P \propto f(r_1) g(p_T, y)$, where the radial profile function

$$f(r_1) \propto \left(1 - \frac{r_1^2}{R_T^2}\right)^\alpha \theta(R_T - r_1), \quad (13)$$

with $\alpha = 0.5$ [13] and the momentum distribution $g(p_T, y)$ is left unspecified because it cancels out from the expression of the net survival probability in colour screening scenario defined by

$$S = \frac{\int_0^{R_T} dr_1 r_1 f(r_1) \int_{-L_1/2}^{L_1/2} dz_1 \int_{-\phi_{max}}^{\phi_{max}} d\phi_1}{\int_0^{R_T} dr_1 r_1 f(r_1) \int_{-L_1/2}^{L_1/2} dz_1 \int_{-\pi}^{\pi} d\phi_1}, \quad (14)$$

which can be simplified as

$$S = \frac{2(\alpha + 1)}{\pi R_T^2 L_1} \int_0^{R_T} dr_1 r_1 \left\{1 - \left(\frac{r_1}{R_T}\right)^2\right\}^\alpha \int_{-L_1/2}^{L_1/2} dz_1 \phi_{max}(r_1, z_1). \quad (15)$$

In contrast to our previous paper [12] above expression contains a non-trivial integration on z_1 coordinate.

Often experimental measurement of S at given N_{part} or y is reported in terms of the p_T integrated yield ratio (nuclear modification factor) over the range $(p_T)_{min} \leq p_T \leq (p_T)_{max}$ whose theoretical expression would be

$$\langle S \rangle = \frac{\int_{(p_T)_{min}}^{(p_T)_{max}} dp_T S}{\int_{(p_T)_{min}}^{(p_T)_{max}} dp_T}. \quad (16)$$

So far we have discussed about the suppression of directly produced J/ψ . However, it is well established fact that only about 60% of the observed J/ψ originate directly in hard collisions while 30% of them come from the decay of χ_c and 10% from the ψ' . Hence, the p_T integrated survival probability $\langle S \rangle$ of J/ψ in the QGP becomes

$$\langle S \rangle = 0.6 \langle S \rangle_\psi + 0.3 \langle S \rangle_{\chi_c} + 0.1 \langle S \rangle_{\psi'}. \quad (17)$$

Now let us turn towards the numerical section of our work.

3 Numerical Work

Table 1 gives the values of various parameters used in our theory and the following explanations are relevant in this context. The value $T_c = 0.17$ GeV is in accordance with lattice QCD results [1]. The choice $c_s^2 = 1/3$ is most common for free massless partons in an ideal gas, although for partons which carry thermal mass or interact among themselves c_s^2 may be different like $1/5$. The selection $\beta = 1$ [13] indicates that the energy deposited in the collision is proportional to the number of nucleon-nucleon collisions. The initial proper time τ_i for QGP thermalization is taken as 0.6 fm/c in accord with [26, 30]. Also, relevant properties of the various quarkonia in a thermal medium are displayed in Table 2. It is clear that the dissociation temperature T_D gradually decreases in going from J/ψ to χ_c to ψ' .

As regards the length L_1 of the primordial cylinder (in $c = \hbar = 1$ units) the Lorentz contracted total radius of the Au+Au system gives a very small value $\sim 2 R_{Au}/200 \sim 0.070$ fm. The alternative estimate based on primordial creation time is also equally small namely, $\tau_1 \sim 1/2m_c \sim 0.066$ fm/c which, however, can be made more logical by remembering that the corresponding longitudinal locations of the created $c\bar{c}$ pairs are expected to be of the order $|z_1| \sim \tau_1 \sinh(|y|)$. Here y is the rapidity whose experimentally determined bin reported in PHENIX experiment is $1.2 \leq |y| \leq 2.2$. Hence the length L_1 of the cylinder is expected to lie in the range $0.10 \leq L_1 \leq 0.29$ so that its approximate mid value $L_1 \sim 0.2$ fm can be used. A detailed but unknown dependence of L_1 on N_{part} will not be attempted because we do not want to keep adjustable free parameters in the analysis.

Our numerical procedure proceeds through the following steps:

- (i) Before finding the centrality (or impact parameter) dependence of J/ψ suppression it is necessary to know the initial average energy density $\langle \epsilon \rangle_i$ in terms of the number of participants N_{part} . For this purpose, we extract the transverse overlap area A_T and the pseudo-rapidity distribution $(dE_T/d\eta_H)_{\eta_H=0}$ reported in ref. [31] at various values of number of participants N_{part} . These $(dE_T/d\eta_H)_{\eta_H=0}$ numbers are then multiplied by a constant Jacobian 1.25 to yield the rapidity distribution $(dE_T/dy_H)_{y_H=0}$ occurring in (5).
- (ii) The original Bjorken formula although provides an estimate of the initial energy density qualitatively yet, unfortunately, it under-estimates the initial energy density which can cause the suppression of only χ_c and ψ' but not of J/ψ . Hence, a scaling-up factor $\xi = 5$ has been introduced in (5) in order to obtain the desired $\langle \epsilon \rangle_i = 45$ GeV/fm³ [30] for most central collision. Of course, this choice of ξ works for other values of N_{part} also. The appropriate characterization of kinematic quantities in Au+Au collisions is presented in Table 3. The relatively large values of our $\langle \epsilon \rangle_i$ have the following justification: These are consistent with the predictions of the self-screened parton cascade model [32], these agree with the requirements of hydrodynamic simulation [30] which describes the pseudo-rapidity distribution of charged particle multiplicity $dN_{ch}/d\eta_H$ for various centralities already observed at RHIC, and these can cause melting of all the quarkonium species listed in Table 2.
- (iii) Next, we calculate the time $\tilde{\tau}_{s0}$ for the pressure to drop to P_s at the origin and thereby deduce the screening radius r_s with the help of (8,9,10,11) for J/ψ mesons of given p_T and y .
- (iv) Next, the quantity Y is computed from (12) which sets the condition for the quarko-

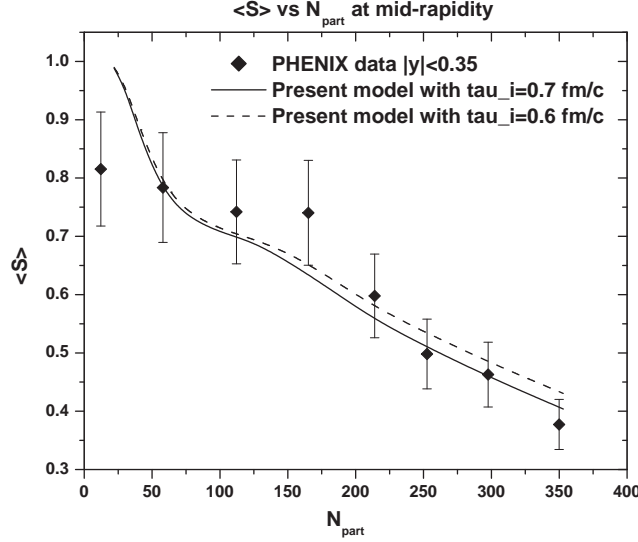


Figure 1: The variation of p_T integrated survival probability $\langle S \rangle$ in the range allowed by invariant p_T spectrum of J/ψ measured by PHENIX experiment, versus number of participants at mid-rapidity predicted by our present model. Corresponding experimental data of J/ψ suppression with respect to N_{part} at [9, 26, 28] have also been shown for comparison.

nium to escape from the screening region, and the limiting values of the $\phi_{max}(r_1, z_1)$ are constructed using equation written just below (12).

(v) Finally, the survival probability S , at specified y and fixed p_T but varying N_{part} is evaluated by Simpson quadrature from (15) from which p_T integrated $\langle S \rangle$ is also deduced.

(vi) The same numerical process is used to calculate the $\langle S \rangle$ for all other higher quarkonia and finally, by including sequential melting of higher resonances, total $\langle S \rangle$ has been calculated from (17).

(vii) In order to compare the above analysis with the actual experimental data it is necessary to convert the J/ψ suppression data available in terms of nuclear modification factor R_{AA} [9] into the accepted def. of survival probability S [26, 28] namely

$$S = \frac{R_{AA}}{R_{AA}^{CNM}}, \quad (18)$$

where R_{AA} is the standard nuclear modification factor and R_{AA}^{CNM} is a contribution to R_{AA} originating from CNM effects constrained by the data of $d + Au$ collisions.

Now we turn to physical interpretations of our results.

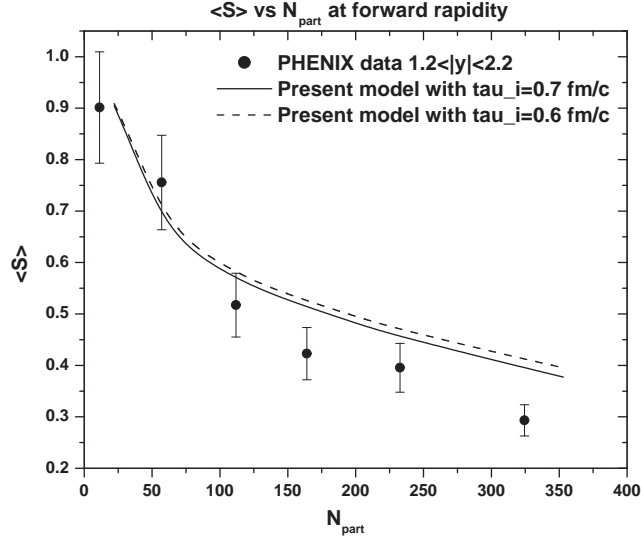


Figure 2: Same as Fig. 1 but at forward rapidity [9, 28].

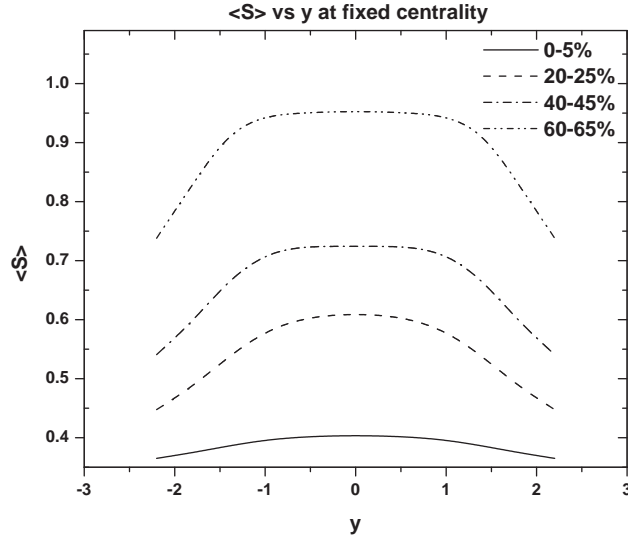


Figure 3: Graph showing the theoretical variation of p_T integrated survival probability i.e., $\langle S \rangle$ with respect to rapidity y at fixed centralities when initial proper time τ_i for QGP thermalization is 0.7 fm/c.

Table 1: Various parameters used in the theory.

T_c (GeV)	c_s^2	B (GeV/fm ³)	P_s (GeV/fm ³)	β	α	τ_i (fm/c)
0.17	1/3	0.405	9.39	1	0.5	0.6, 0.7

Table 2: Masses, formation times and dissociation temperatures of J/ψ , χ_c and ψ' [4].

	J/ψ	χ_c	ψ'
m (GeV)	3.1	3.5	3.7
τ_F (fm)	0.89	2.0	1.5
T_D/T_c	2.1	1.16	1.12

Table 3: Kinematic characterization of Au+Au collisions at RHIC [9].

Nuclei	$\sqrt{s_{NN}}$ (GeV)	ξ	N_{part}	$\langle \epsilon \rangle_i$ (GeV/fm ³)	R_T (fm)
Au+Au	200	5.0	22.0	5.86	3.45
			30.2	7.92	3.61
			40.2	10.14	3.79
			52.5	12.76	3.96
			66.7	15.69	4.16
			83.3	18.58	4.37
			103.0	21.36	4.61
			125.0	24.38	4.85
			151.0	27.37	5.12
			181.0	30.52	5.38
			215.0	34.17	5.64
			254.0	37.39	5.97
			300.0	41.08	6.31
			353.0	45.09	6.68

4 Results and Discussions

We present our numerical results as follows:

Figures 1 and 2 show the variation of p_T integrated values of the survival probability $\langle S \rangle$ with respect to number of participants N_{part} at mid and forward rapidities, respectively. The two curves on each figure correspond to experimental data (solid circles) and our model predictions (solid and dashed lines). It is obvious from the Figures that $\langle S \rangle$ decreases with increase in N_{part} both experimentally and theoretically because of the increase in the energy density with respect to N_{part} . Moreover, the agreement between the experimental data and the prediction of our present model is remarkable. This lends support to our use of the pressure parametrization containing bag constant B . A satisfying feature of Figures 1 and 2 is that our model prediction for $\langle S \rangle$ is obtained by simply inserting the relevant values of the rapidity y in contrast to other model [25] where different additional parameters are needed for describing the data in different rapidity bins.

However, It must be emphasized in context of Figures 1 and 2 that the physics at mid and forward rapidities has the following important distinctions:

- (i) Although the quality of fit between our model and experimental data is excellent for mid-rapidity data yet it worsens somewhat for forward rapidity. This may be attributed to the fact that our present formulation is based on the assumption of Bjorken's boost invariant longitudinal expansion, which requires cylindrical symmetry about the collision axis. This cylindrical symmetry may be violated up to some extent for most forward rapidities.
- (ii) There would be more uncertainties in normalizing the nuclear modification factor by Glauber suppression factor, while extracting the J/ψ suppression due to normal nuclear matter, at forward rapidity in the PHENIX experiment.
- (iii) As pointed out beneath (11) the radius r_s of the deadly region at higher rapidity is larger than that at lower rapidities. Therefore, for a J/ψ meson of given p_T , the transversal time will also be correspondingly larger implying that the predicted survival probability must decrease with increasing $|y|$. This fact is clearly seen in Fig. 3 where we have displayed the variation of $\langle S \rangle$ with respect to rapidity y at fixed centrality i.e., N_{part} . It is clear from this figure that $\langle S \rangle$ shows peak around $|y| \approx 0$ and decreases at higher $|y|$. This agrees well with the experimental data at RHIC [9, 26, 28].

It should be noted that our model does not involve any free parameter although there are some parameters used in the calculation. We have assigned proper justifications to their values and these values are also used in other calculations e.g., in Chu and Matsui model [13] and hydrodynamical models [26, 30]. Moreover, our result do not depend significantly on the values of the parameters used here. For example, we have shown in Fig. 1 and 2, the results of calculations when the initial proper time for QGP thermalization is $\tau_i = 0.7$ fm/c. We find that the results do not change much.

5 Summary and Conclusions

Generalization of our previous work [12], based on the J/ψ +hydro framework involving (1+1)-dimensional expansion of Chu and Matsui [13] model, has been done in the present

paper in order to incorporate complete rapidity dependence of the J/ψ suppression. The present work also takes into account the additional time dilatation effect for charmonium formation due to its transverse motion and this makes our model different than the calculation by Gunji et al. [26]. Our formulation shows explicit dependence of the J/ψ suppression on transverse momentum, centrality as well as on the rapidity and the predictions are consistent with the data. Our model has suitably incorporated the results from recent lattice simulation on the dissociation temperature and formation time of J/ψ , as well as on the sequential melting of higher resonances. We have analyzed the centrality dependence of the J/ψ suppression data available from RHIC in terms of the survival probability versus number of participants at mid-rapidity as well as at forward rapidity. We have also presented here the rapidity dependence of the J/ψ suppression at fixed centrality and our results show agreement with the experimental data. Our results reproduce the main feature of the PHENIX data as we observe more suppression at forward rapidity as compared to mid-rapidity region and this is in a very good agreement with the recent PHENIX data. It is creditable to notice that the same mechanism explains the suppression patterns observed in the entire rapidity regions. Further extension of this work, such as incorporation of (3+1)-dimensional hydrodynamic expansion and the predictions of our model at LHC energies would provide further support to our ideas.

Acknowledgements

M. Mishra and V. J. Menon are grateful to the Council of Scientific and Industrial Research (CSIR), New Delhi for their financial assistance.

References

- [1] T. Hatsuda, J. Phys. G **34** (2007) S287.
- [2] T. Matsui and H. Satz, Phys. Lett. B **178** (1986) 416.
- [3] S. Dutta, F. Karsch, P. Petreczky and I. Wetzorke, Phys. Rev. D **69** (2004) 094507.
- [4] H. Satz, J. Phys. G **32** (2006) R 25.
- [5] M. J. Tannenbaum, Rep. Prog. Phys. **69** (2006) 2005;
C. P. Singh, Phys. Rep. **236** (1993) 147;
B. Müller and J. L. Nagle, Annu. Rev. Nucl. Part. Sci. **56** (2006) 93.
- [6] M. C. Abreu et al., Phys. Lett. B **410** (1997) 337.
- [7] B. Alessandro et al., Eur. Phys. J. C **39** (2005) 335.
- [8] M. C. Abreu et al., (NA50 Collaboration), Phys. Lett. B **477** (2000) 28.
- [9] A. Adare et al., (PHENIX Collaboration), Phys. Rev. Lett. **98** (2007) 0232301.
- [10] Xiao-Ming Xu, D. Kharzeev, H. Satz and Xin-Nian Wang, Phys. Rev. C **53** (1996) 3051.
- [11] B. K. Patra and V. J. Menon, Eur. Phys. J. C **37**, (2004) 115;
B. K. Patra and V. J. Menon, Eur. Phys. J. C **48**, (2006) 207.
- [12] M. Mishra, C. P. Singh, V. J. Menon and R. K. Dubey, Phys. Lett. B **656** (2007) 45.
- [13] M. C. Chu and T. Matsui, Phys. Rev. D **37** (1988) 1851.
- [14] L. Grandchamp, R. Rapp and G. E. Brown, Phys. Rev. Lett. **92** (2004) 212301.
- [15] A. Andronic, P. Braun-Munzinger, K. Redlich and J. Stachel, Phys. Lett. B **571** (2003) 36.
- [16] R. L. Thews and M. L. Mangano, Phys. Rev. C **73** (2006) 014904;
R. L. Thews, Nucl. Phys. A **783** (2007) 301.
- [17] S. S. Adler et al., Phys. Rev. Lett. **96** (2006) 032301.
- [18] A. Adare et al., Phys. Rev. Lett. **97** (2006) 252002.
- [19] S. S. Adler et al., (PHENIX Collaboration), Phys. Rev. Lett. **96** (2006) 012304.
- [20] A. Capella, E. G. Ferreira and A. B. Kaidalov, Phys. Rev. Lett. **85** (2000) 2080.
- [21] A. P. Kostyuk, M. I. Gorenstein, H. Stöcker and W. Greiner, Phys. Rev. C **68** (2003) 041902.
- [22] M. I. Gorenstein, A. P. Kostyuk, H. Stöcker and W. Greiner, Phys. Lett. B **509** (2001) 277.

- [23] A. Andronic, P. Braun-Munzinger, K. Redlich and J. Stachel, Phys. Lett B **652** (2007) 259.
- [24] A. K. Chaudhuri, Phys. Rev. C **74** (2006) 044907.
- [25] A. K. Chaudhuri, Phys. Lett. B **655** (2007) 241.
- [26] T. Gunji, H. Hamagaki, T. Hatsuda and T. Hirano, Phys. Rev. C **76** (2007) 051901.
- [27] F. Karsch, D. Kharzeev and H. Satz, Phys. Lett. B **637** (2006) 75.
- [28] Raphaël Granier de Cassagnac, hep-ph/0701222 (2007).
- [29] A. Chodos, R. L. Jaffe, K. Johnson, C. B. Thorn and V. F. Weisskopf, Phys. Rev. D **9** (1974) 3471; K. Johnson, A. Chodos, R. L. Jaffe and C. B. Thorn, Phys. Rev. D **10** (1974) 2599.
- [30] T. Hirano, Phys. Rev. C **65** (2001) 011901;
T. Hirano and K. Tsuda, Phys. Rev. C **66** (2002) 054905.
- [31] S. S. Adler et al., (PHENIX Collaboration), Phys. Rev. C **71** (2005) 034908;
S. S. Adler et al., (PHENIX Collaboration), Phys. Rev. C **71** (2005) 049901.
- [32] K. J. Eskola, B. Müller and X. N. Wang, Phys. Lett. B **374** (1996) 20.